Automatic Visual Inspection Machine for Pharmaceutical Infusion Bags Implementing Cellular Neural Networks

Automatic Visual Inspection Machine for Pharmaceutical Infusion Bags Implementing Cellular Neural Networks

Francesco Marrone*, Gianluca Zoppo*, Luca Vescovi†, Filippo Begarani†, Ada Palamà*,
Jacopo Secco* and Fernando Corinto*
*Department of Electronics and Telecommunications
Politecnico di Torino, Torino, Italy
Email: (francesco.marrone)(gianluca.zoppo)(ada.palama)(jacopo.secco)(fernando.corinto)@polito.it
†Department of R&D
PBL srl, Rubbiano (PR), Italy
Email: (luca.vescovi)(filippo.begarani)@pblsrl.it

***Abstract*—Automation procedures and machines in the pharmaceutical field are required to implement a series of methodologies, designed parting from international standards, in order to ensure the high quality of the products. Regarding infusion bags, the standards require to thoroughly assess the conformity of the product before being used in patients. The inspection procedures are usually operator-based and therefore subject to human factor errors. A novel inspection machine has been designed and developed with the use of a specifically designed cellular neural network (CNN) coupled with an *off-the-shelf* neural network trainable solution. The novel machine, thanks to the computational versatility of the CNN, is capable of reaching high standards of assessment drastically decreasing the risk of operator-based errors in the procedure.**

***Index Terms*—cellular neural network, neural network, pharmaceutical inspection, infusion bags, automation**

I. Introduction

The injection of therapeutics is a common medical procedure. Venous drug administration leads to a more rapid effect of the medicament on the system and to a mitigation of pharmacokinetic risks driven by other means of delivery (i.e. oral administration). Intravenous injections are obviously subject to administration errors both due to preparation mistakes and human error [1]. Preparation errors do not only occur in the preparation of the solution to be injected, but also in their packaging procedure. In the production process, pharmaceutical companies must implement very strict procedures regarding the inspection of the bottles or the bags in which the drug is contained. Due to the preparation of the packages and the nature of the material of which they are made of, it is possible to find various inclusions suspended in the solution to be injected such as glass or polymer fragments, dirt or other solid state particles (all these henceforth generically named as defects) [2]. The presence of defects in the drug containers can cause severe damages to the patients: infections, high inflammatory response, or in the worst cases it can lead to death [3].

As afore mentioned, the scrutiny tests for detecting invalid packages must be put into action before the drug is delivered to the hospitals for clinical use. The screening is nowadays normally performed manually by human operators which are allowed, illuminating the bag and imprinting a movement of the liquid to enhance the defect's visual characteristics [4]. Due to its implications, the work of the visual inspectors for infusion packages is considered a drudgery, but still of high importance since the need for infusional drugs has drastically increased in recent times as a result of the COVID-19 pandemic. For this reasons several research groups, facilities and companies have developed different technological solutions to overcome the problem [2], [5]–[7]. The solution presented in this paper is intended to provide a fully equipped visual inspection machine capable of automatically recognizing and classifying the defects. It has been designed to perform the inspection without the intervention of the operator and to be implemented in a large scale pharmaceutical production line.

To perform the inspection, the machine captures a series of digital images of the filled package, illuminated from different light sources, that are then processed with a CNN [8] coupled with an *off-the-shelf* trainable neural network solution [9]. The implemented CNN has the scope to perform a well defined series of image processing steps in order to enhance the features of the objects that have to be detected. This has been done, as it will be described in details in the following sections of this work, exploiting the equivalence between a *cellular automaton* [10] and a *discrete-time cellular neural network* (DT-CNN) [11], [12]. The second network is coupled in a waterfall configuration with the CNN and is divided in two sub-networks. The first is composed by 24 of convolutional layers, responsible for the feature extraction of the different defect classes that the network is trained to detect, the second is composed by two fully connected layers that serve for inferential prediction of the results (see [9]

978-1-6654-3948-0/21/$31.00 ©2021 IEEE

for further information). The machine was trained to identify three classes of defects with different light reflection and dynamical properties in fluids. The efficiency of the system was tested through a Knapp test which is normally carried out to, dictated by U.S. FDA and European Pharmacopoeia, ensure that normal manual inspection standards are met also by automatic methodologies [13], [14] resulting in an over 90% identification rate for all three defect classes.

As shown in other recent works [15], [16], CNNs have been exploited as a valid tool for image processing, pattern recognition and feature extraction. In the presented work, the *ad hoc* designed network resulted to be a key player in the inspection process, enhancing the defects' morphological and dynamical features rendering and enabling more complex networks able to reach high standards of recognition. The proposed machine is a novel example of real-life industrial application of such technology, since its implementation in pharmaceutical production lines has already contributed in increasing the quality of the production, mitigating the risks attributable to human error.

II. Machine and Inspection Procedure Description

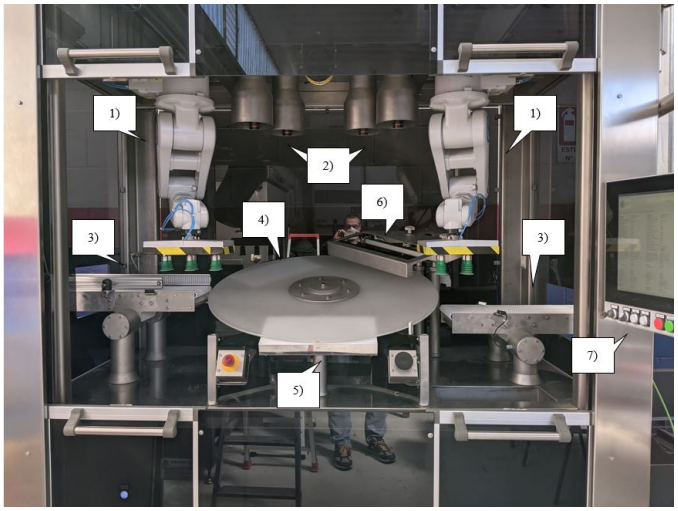

Figure 1. Picture of the finished machine showing its functional mechanical and computational components. 1) Robotic arms (ABB®) equipped with six air vacuum suction cups for package transportation - 2) Four digital cameras (Matrix Vision®) set to capture $13fps$ at a resolution of 1600×768 - 3) Package inlet and outlet conveyor belts - 4) Mechanical transparent disk carousel - 5) Transmission lighting source - 6) Lateral lighting source - 7) user interface and computational station (equipped with an Intel®i7, 6-core, 12-thread, $24GB$-RAM CPU and a Nvidia®GTX 2080 $8GB$-RAM GPU).

The inspection machine that has been built and developed is shown in Figure 1. The figure reports a short description of the main functional components of the system that are involved in the automated inspection procedure. The system has been designed in order to be integrated in a full scale production line. For this reason the machine has been set to perform twenty to thirty inspections every minute.

As afore mentioned, the screening of the products is completely automated and does not require the direct intervention of the operator, even though this kind of event has been provided as a standard requirement. During a normal production process each bag enters the machine through the inlet conveyor belt and its arrival is sensed through a standard IR proximity sensor. The first of the two mechanical arms is then activated picking up the product and deploying it on the disk mechanical carousel which produces a $45°$ spin positioning the package over the transmission lighting source. The spin imprints a movement to the solution contained in the bag inducing eventual defects change their initial position. The first set of cameras (two cameras are required in order to ensure the complete view of the package) take a set of 13 pictures of the product with the settings described in the caption of Figure 1, while a second package is positioned on the carousel. With a second $45°$ spin the carousel imprints a new movement to the contained liquid solution and to the defects positioning it in proximity of the lateral lighting source. At this stage another set of 13 pictures is taken by the second set of cameras. The two sets of pictures taken to the bags with different illuminations have the scope to increase the visibility of the inclusions which depend on their morphological and reflective characteristics (for instance, transparent defects are more visible when illuminated by a lateral light source). Finally the two sets of images are sent to the computational station where the actual screening takes place on both sets separately in the following order:

1) A pre-processing step taking into account the information from all the 13 images in each set with the use of the designed CNN for feature enhancement described in details in II-A;
2) A feature extraction and object recognition procedure through the waterfall-coupled neural network [9].

If a defect is detected in at least one frame of the two sets the second arm will extract the package deploying it in the discard bin for further control. If the bag is considered to be compliant to the required standards, the robotic arm will deploy the product on the outlet conveyor belt.

It is necessary to note that the second neural network is capable of correctly identifying the desired objects and classify them only after a specific training session of the system on the different defect classes. The training set is built with the same procedure of the inspection including the step of the feature enhancement through the CNN. The required bounding boxes are inserted manually by trained operators (see [9] for the detailed training procedure). The trained network is then saved on the machine's CPU and can be updated regularly when new defects are found in the inspection process through the same procedure.

A. Feature Enhancement Through CNN

As introduced in Section I, the CNN that has been developed and implemented in the machine, was designed to work as a DT-CNN [11], [12]. The network is composed by a two-dimensional layer of locally connected cells with same dimension of the images that are processed. All the cells at every epoch, or computational iteration, change their internal

state according to their initial condition and the states of the cells that reside inside a preset neighborhood according to:

$$\frac{dx_{i,j}}{dt} = -\gamma x_{i,j} + \sum_{k,l \in N_{i,j}} (a_{k,l} y_{k,l} + b_{k,l} u_{k,l}) + z_{i,j}. \quad (1)$$

In Equation 1, $x_{i,j}$ and $y_{i,j}$ represent the input (initial condition) and output states respectively of the i^{th} and j^{th} cell of the N network, while $a_{k,l}$ and $b_{k,l}$ represent the elements of the feedback A and feedforward B templates of the k^{th} and l^{th} neighbour cells. γ is a conversion factor (that for this application has been set to 1), $u_{k,l}$ is a step function operator of $x_{k.l}$, $z_{i,j}$ is the current matrix or a constant correction factor that depends on the desired operator.

Templates A and B (which referring to Equation 1, in Figure 2 are shown presenting the results of each passage) determine the actual dynamics of the internal state changes of the cells and have been calculated on the basis of the here described application. Under a functional point of view it must be taken into account that the images captured by the two camera sets are in tones of grey ($256B$) and the defects that have to be detected of the same class might have heterogeneous morphological features. On the other hand, the bags might contain bubbles that can be detected as defects by the feature extraction neural network. For this reason the CNN was designed to implement the following strategy enhancing other features that can differentiate the detected defects during the scrutiny.

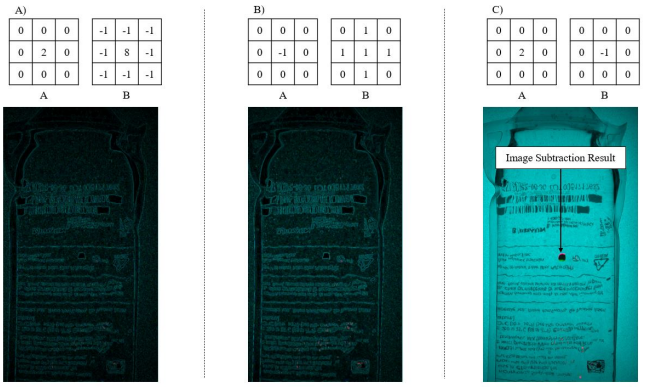

Figure 2. Image analysis steps for feature enhancement performed by the CNN and relative results. A) Edge detection and binarization - B) Dilation - C) Image subtraction. In C) is also highlighted the result of the image subtraction that shows that the difference between the two frames of the sequence correpond to the movement of the defect that was found in the bag.

1) At first, each image of every sequence is analyzed with the scope of determining the edges of every visible object from the bag. Referring to Figure 2-A the result of the processing highlights both the defect edges and the edges of all the other visible features of the bag (i.e. bubbles, writings and bag borders).
2) The second image processing activity consists of a dilation of the edges (Figure 2-B).
3) At last, the results of the dilation is subtracted from the dilation of the edges of the preceding image of the sequence. As can be noted from Figure 2-C, this induces the deletion of the visible objects that are standard for every bag (i.e. writings and labels) and the enhancement of the trajectories of the other objects that reside in the solution contained in the bag (i.e. bubbles and defects). Referring to Equation 1, in this particular step, the initial conditions of the cells $x_{i,j}$ are given by the input image, while the values of the pixels of the preceding image substitute the respective values of $u_{k,l}$.

As a last step the result of the CNN feature enhancement is exploited as a mask which is overlapped to the original image coming form the camera sets. Before performing the overlap, the result of the CNN processing is digitally modified in order to render it with a 50% transparency as shown in Figure 3-A.

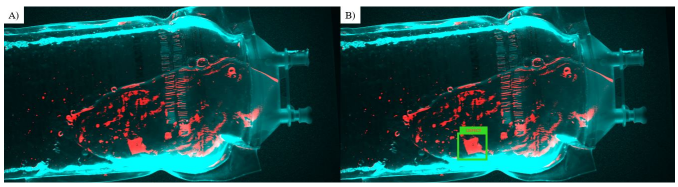

Figure 3. Results of the A) CNN feature enhancement and B) object detection performed by the coupled neural network.

B. Feature Extraction and Testing

The feature enhancement technique explained in II-A provides additional information regarding the elements contained in the bag. The additional features are represented by the trajectories of the same elements: both bubbles and defects. As it has been noted during the development process of the machine defects and bubbles differ, a part from shape and light transparency, by their dynamical behaviour when immerged in liquids with known characteristics. Moreover, their dynamical behavior increases the capabilities of the coupled neural network in distinguishing the different defect classes for which the network is trained to recognize.

For the machine test, three different kinds of defects were used: a black paper defect with $0.5 \times 0.5cm^2$ size, a $0.3 \times 0.3cm^2$ aluminium foil and an almost transparent plastic $0.5 \times 0.5cm^2$ fragment. Each defect was inserted singularly in ten bags (all with the same writings and labeling) filled with a water solution, while ten bags were left without defect. To train the feature extraction network twenty of the fifty bags were randomly chosen and were passed inside the machine which took the two different sets of 13 images with the two different illumination setups (transmission and lateral lighting sources). All the sequences were processed through the CNN for feature enhancement as described in details in II-A. Differently form the normal operative procedures of the machine, the images were not assessed by the second network, but the processed images were stored. In a second phase, all the images were shown in sequence to a trained operator who digitally drew a bounding box whenever he was able to see a defect in a given

image: the bounding box had to include both the defect and its trajectory highlighted by the CNN processing (as showed in Figure 3-A). The data regarding the processed images and the traced bounding boxes were given to the second neural network for feature extraction (see [9] for detailed training procedure).

Once the system was trained to recognize and the three different kinds of defects, the trained network was saved in the computational unit of the machine (Figure 1-3). The machine was tested using the standard procedures of the Knapp Test [13], [14]. In synthesis each of the prepared 40 bags was passed in the machine for the automatic screening ten times each. The test is considered to be passed (i.e. the automatic screening of the bags methodology is considered to be equivalently efficient as the operator based analysis) if in more than 70% of the cases the defects were detected. In case the analysis is performed on a defect-less bag, the test is considered to be passed with a false positive score lower than 30%. Every time a bag with a defect was assessed with the machine, a second opinion from a trained operator was always required: for this reason the object detection results were shown to the operator thorough the user interface of the system. When a defect was detected (see [9] for further reference) is shown on screen as the example depicted in Figure 3-B.

Table I
KNAPP TEST RESULTS FOR DIFFERENT DEFECT TYPES

Defect	No. Runs/Bag	True Pos./Neg.	False Pos./Neg.
Defect-less	**10**	98%	2%
Black paper	**10**	95%	5%
Aluminium foil	**10**	93%	7%
Transp. plastic	**10**	88%	12%

The results of the Knapp Test are reported in Table I. From the table is possible to note that the percentage of the obtained false positives (in case of defect-less bags) and false negatives are lower than the required upper limit of 30% given by the test standards resulting that the machine is capable of being implemented in a normal large scale production line. Even though the test had a successful outcome, the worst results were obtained in the scrutiny of bags which had the transparent plastic defect. This is due to the fact that this kind of inclusion is not always visible when enlightening the bag with transmission light. This leaves the object detection only to the images that were taken with lateral lighting. This is a common problem also for the operator-based inspections, but the proposed solution was able to obtain a high standard of recognition even in presence of this impediment.

III. CONCLUSIONS

This work is a further demonstration of the obtainable analysis efficiencies when exploiting CNNs in a real life case. Moreover their reliability has been proven in this particular example where high analysis precision is required due to the possible high clinical impacts of procedural errors. The CNN network, coupled with a feature extraction methodology rendered the system a valuable example of production efficiency which is already stably in use in a large scale scale production facility.

ACKNOWLEDGMENT

The authors would like to thank Franco and Marco Serventi, and all the PBL srl R&D team for their support and their cooperation in this work.

REFERENCES

[1] V. Wirtz, N. Barber *et al.*, "An observational study of intravenous medication errors in the united kingdom and in germany," *Pharmacy World and Science*, vol. 25, no. 3, pp. 104–111, 2003.

[2] Q. Wang, H. Zhang, L. Liu, H. Zhong, Y. Wang, and Q. J. Wu, "The automatic liquid particles detection for injection," in *2020 Chinese Automation Congress (CAC)*. IEEE, 2020, pp. 6039–6044.

[3] S. E. Langille, "Particulate matter in injectable drug products," *PDA J Pharm Sci Technol*, vol. 67, no. 3, pp. 186–200, 2013.

[4] C. P. Commission *et al.*, "Chinese pharmacopoeia," *China Medical Science Press: Beijing, China*, vol. 1, pp. 191–193, 2015.

[5] H. Zhang, X. Li, H. Zhong, Y. Yang, Q. J. Wu, J. Ge, and Y. Wang, "Automated machine vision system for liquid particle inspection of pharmaceutical injection," *IEEE Transactions on Instrumentation and Measurement*, vol. 67, no. 6, pp. 1278–1297, 2018.

[6] Y. Wang, J. Ge, H. Zhang, and B. Zhou, "Intelligent injection liquid particle inspection machine based on two-dimensional tsallis entropy with modified pulse-coupled neural networks," *Engineering Applications of Artificial Intelligence*, vol. 24, no. 4, pp. 625–637, 2011.

[7] H. Grindinger, H. Neusser, N. Seidenader, and V. Wedershoven, "Product testing apparatus," Jun. 2 2005, uS Patent App. 10/928,433.

[8] L. O. Chua and L. Yang, "Cellular neural networks: Theory," *IEEE Transactions on circuits and systems*, vol. 35, no. 10, pp. 1257–1272, 1988.

[9] J. Redmon, S. Divvala, R. Girshick, and A. Farhadi, "You only look once: Unified, real-time object detection," in *Proceedings of the IEEE conference on computer vision and pattern recognition*, 2016, pp. 779–788.

[10] S. Wolfram, "Cellular automata as models of complexity," *Nature*, vol. 311, no. 5985, pp. 419–424, 1984.

[11] M. Itoh and L. Chua, "Memristor cellular automata and memristor discrete-time cellular neural networks," in *Handbook of Memristor Networks*. Springer, 2019, pp. 1289–1361.

[12] H. Harrer and J. A. Nossek, "Discrete-time cellular neural networks," *International Journal of Circuit Theory and Applications*, vol. 20, no. 5, pp. 453–467, 1992.

[13] J. Z. Knapp, "The scientific basis for visible particle inspection," *PDA Journal of Pharmaceutical Science and Technology*, vol. 53, no. 6, pp. 291–302, 1999.

[14] J. Z. Knapp and H. K. Kushner, "Generalized methodology for evaluation of parenteral inspection procedures," *PDA Journal of Pharmaceutical Science and Technology*, vol. 34, no. 1, pp. 14–61, 1980.

[15] J. Secco, M. Farina, D. Demarchi, F. Corinto, and M. Gilli, "Memristor cellular automata for image pattern recognition and clinical applications," in *2016 IEEE International Symposium on Circuits and Systems (ISCAS)*. IEEE, 2016, pp. 1378–1381.

[16] G. Zoppo, F. Marrone, M. Pittarello, M. Farina, A. Uberti, D. Demarchi, J. Secco, F. Corinto, and E. Ricci, "Ai technology for remote clinical assessment and monitoring," *Journal of wound care*, vol. 29, no. 12, pp. 692–706, 2020.